

## Noon-time equatorial electrojet: Its spatial features as determined by the CHAMP satellite

H. Lühr, S. Maus, and M. Rother

GeoForschungsZentrum Potsdam, Potsdam, Germany

Received 21 August 2002; revised 7 October 2003; accepted 4 November 2003; published 24 January 2004.

[1] New observations obtained by the satellite CHAMP reveal a detailed picture of the noon-time equatorial electrojet (EEJ). The low orbit of CHAMP and its high-precision magnetometers reveal the spatial structure of the EEJ with unprecedented accuracy. Data from more than two and a half years have been used to investigate average features and also the global characteristics of the EEJ. Rather than interpreting the magnetic signatures, we determined the horizontal current distribution by using a very general current model (series of line currents). This makes the results independent of satellite altitude and ambient field geometry. The procedure for determining the structure of the electrojet is fully automated, giving an objective response. Some of the spatial features of the noon-time EEJ are as follows: The electrojet current peaks right at the dip equator. There is no deviation from it either on a seasonal basis or with longitude. The width of the EEJ ( $\approx 4^\circ$  in latitude) at half the peak value of the current density profile is for a given longitude fairly constant, independent of the amplitude. Return currents north and south of the eastward current are a common feature of the EEJ. They peak at latitudes some  $5^\circ$  away from the dip equator. The intensity of the EEJ varies strongly from day to day. The average peak current density exhibits a clear dependence on longitude. Peaks show up over South America and Indonesia. The average current density follows closely the monthly mean of the solar flux index, F10.7. The total EEJ eastward current is about three times as strong as the return current. The total current and the peak current density are related to each other by a power law. This suggests that the longitude dependence of the EEJ intensity can be explained by the varying cross-sectional area of the Cowling channel. **INDEX TERMS:** 2409 Ionosphere: Current systems (2708); 2415 Ionosphere: Equatorial ionosphere; 2427 Ionosphere: Ionosphere/atmosphere interactions (0335); 2437 Ionosphere: Ionospheric dynamics; 1555 Geomagnetism and Paleomagnetism: Time variations—diurnal to secular; **KEYWORDS:** equatorial electrojet, ionospheric currents, geomagnetic field

**Citation:** Lühr, H., S. Maus, and M. Rother (2004), Noon-time equatorial electrojet: Its spatial features as determined by the CHAMP satellite, *J. Geophys. Res.*, 109, A01306, doi:10.1029/2002JA009656.

### 1. Introduction

[2] The equatorial electrojet (EEJ) represents a ribbon of intense electric current flowing along the dip-equator in the ionospheric E region on the day-side. The primary reason for the high current density is the geomagnetic field geometry exhibiting horizontal lines of force at these latitudes. Cowling [1933] was the first to recognize that in such a field configuration the Hall current, flowing normal to the boundaries (non-conducting atmosphere at the bottom and effectively collisionless plasma at the top), is restricted, setting up a vertical electric field which in turn causes a significant enhancement of the conductivity (Cowling conductivity) parallel to the boundaries.

[3] There have been many studies investigating the EEJ from ground observations [e.g., Forbes, 1981; Rastogi, 1989], from sounding rockets [e.g., Onwumechili, 1997,

and references therein], and from low-Earth orbiting satellites [e.g., Cain and Sweeney, 1973; Onwumechili and Agu, 1981a; Langel *et al.*, 1993; Jadhav *et al.*, 2002; Ivers *et al.*, 2003]. These three types of measurements are complementary. Ground-based observations track very closely the temporal variations of the electrojet intensity. Rocket measurements provide the only means of in-situ observations of important EEJ parameters like the current density distribution. Low-Earth orbit satellites on the other hand pass very rapidly over the current system. Their measurements thus can be regarded as a snapshot of the spatial structures.

[4] Alongside the interpretation of observations, physical models were developed describing the electrodynamics associated with the EEJ [e.g., Richmond, 1973a, 1973b; Fambitakoye *et al.*, 1976; Ananda Rao and Raghava Rao, 1987]. Although general features of the EEJ are well described by the models, quantitative comparisons show that they do not explain all observations.

[5] In this article we employ magnetic field data from the CHAMP satellite to study the low latitude ionospheric

current systems. The low altitude ( $\approx 430$  km) of the spacecraft and the high resolution instrumentation make this mission particularly suitable for investigating the details of the EEJ. An important prerequisite for a proper interpretation of observed magnetic field features in terms of currents is the effective separation of contributions from other field sources. Here we make use of the latest models of the main field, lithospheric field and large-scale magnetospheric contributions, as derived from the recent high-quality magnetic field missions. In addition we correct the magnetic field readings for the diamagnetic effect caused by the ambient plasma. This ensures highly reliable results.

[6] Rather than interpreting the magnetic signature of the EEJ, we have inverted the readings to estimate the current density distribution in the E region. All subsequent investigations are based on the obtained current profiles. The advantage of this approach, which is different from many previous studies, is that the current density is independent of the measurement height. It allows for direct comparison with observations from other spacecraft or from the ground.

[7] For this initial study we have focused our attention on the noon sector when the EEJ reaches its peak intensity. In this time sector the main currents flow in the east/west direction more or less perpendicular to the geomagnetic field. The meridional current system is expected to be weak becoming more important during the afternoon and evening hours [Langel *et al.*, 1993]. The EEJ is known to be highly variable in its intensity. It varies with longitude, with season, with local time, and on a day-to-day basis. Limiting the study to a certain local time sector helps to understand the remaining variability.

[8] The important questions addressed in this paper concern mainly the spatial features of the EEJ which can be recovered best by satellite measurements. Of particular interest in this context is the latitudinal cross-section through the current system. What is the width of the eastward current? Does it vary on a day-to-day basis [Burrows, 1970], or is the width primarily determined by the geometry of the geomagnetic field at the dip equator [Onwumechili, 1967]? Is there a relationship between EEJ width and current density [Onwumechili and Agu, 1981b]? What is the ratio between the primary forward currents and the return currents? All EEJ parameters show a dependence on longitude [Onwumechili and Agu, 1981a]. Which are the controlling factors for this modulation? A large number of well distributed samples are needed to recover the mean spatial features from the highly variable set of EEJ profiles. Many of these features have been studied in recent papers by Jadhav *et al.* [2002] and Ivers *et al.* [2003] using Ørsted magnetic field data. Our aim is to find out how well previous results can be reproduced with an independent data set.

[9] In the subsequent sections we will first outline our data analysis approach and then present the average characteristics of the EEJ signatures. Subsequently a study of the longitudinal dependence of some EEJ spatial features is performed. Finally we discuss our results in the context of previous publications.

## 2. Data Selection and Processing Approach

[10] For the study presented here CHAMP satellite data have been considered from the period 1 Aug. 2000 through

1 April 2003. Since we are interested in the primary characteristics of the EEJ, we selected data from the hours around noon, 10 to 13 local time when currents are strongest and morning and evening effects can be neglected. Furthermore, only magnetically quiet periods with  $K_p = 0 \dots 2$  have been taken into account. In total 1653 crossings of the equator in the noon sector are considered.

[11] For the determination of the EEJ current distribution we used scalar magnetic field data obtained by the Overhauser magnetometer. The limitation to the field magnitude is justified in this time sector, since the magnetic field caused by the EEJ is well aligned with the ambient field and thus little additional information would be gained by using vector measurements. Magnetic fields are sampled at a rate of 1 Hz and with an accuracy of about 0.1 nT.

[12] The data measured by the magnetometer comprise the sum of contributions from various sources. To isolate the EEJ effect, all the other parts must be removed correctly. We subtracted the field magnitude derived from our recent main field model (Pomme-1.4, <http://www.gfz-potsdam.de/pb2/pb23/SatMag/pomme14.html>).

[13] The POMME 1.4 field model is derived from CHAMP and Ørsted vector data of the years 1999 to 2002. The internal field is represented by Gauss coefficients to degree 15, secular variation to degree 15 (damped for degrees 12–15) and secular acceleration to degree 10 (damped for degrees 7–10). The external field correction includes a ring current field, parameterized by the Dst index. In addition the time-averaged magnetospheric field is modeled by spherical harmonics up to degree 2 in geocentric solar magnetospheric (GSM) coordinates, which is a unique feature of POMME.

[14] Similarly the lithospheric magnetization was accounted for by subtracting an appropriate model (MF2, similar to the one of Maus *et al.* [2002]).

[15] A rather important correction, which is applied for the first time in this kind of study, is the removal of the diamagnetic effect caused by the ambient plasma [Lühr *et al.*, 2003]. For the determination of the local plasma pressure we use the electron density  $n$  measured by the Planar Langmuir Probe (PLP) on board CHAMP, while the ion and electron temperatures are derived from an ionospheric model [Köhnlein, 1986].

[16] A significant modification of the magnetic field readings by this effect is observed in the high plasma density regions of the Appleton anomaly. To correct the deficit in field strength we have used the formula proposed by [Lühr *et al.*, 2003]

$$\Delta B = nk(T_i + T_e) \frac{\mu_0}{B}, \quad (1)$$

where  $n$  is the electron number density,  $k$  the Boltzmann constant,  $T_i$  and  $T_e$  the ion and electron temperatures,  $\mu_0$  the susceptibility of free space and  $B$  the ambient magnetic field magnitude. For  $B$  and  $n$  we have inserted local measurements. The sum of ion and electron temperature, on the other hand has to be estimated. We have chosen a constant value of 2000 K for all events.

[17] The distribution and amplitude of the resulting values of  $\Delta B$ , which have to be added to the field magnitude are shown in Figure 1. Clearly visible are two bands of sizable magnetic field tracking the dip equator and reaching

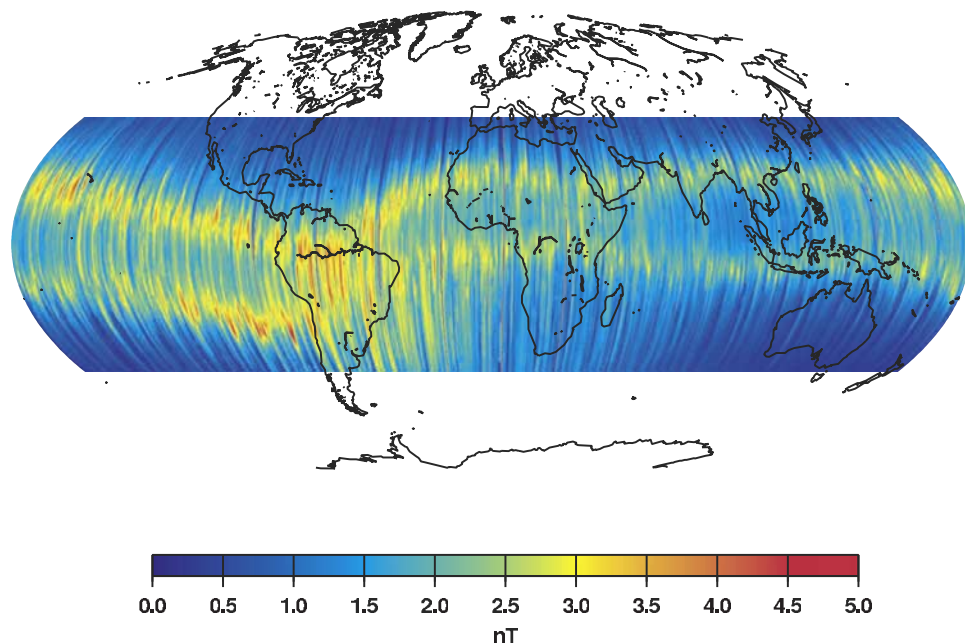


**Figure 1.** Field amplitude and distribution of the correction for the diamagnetic effect applied to our noon-time EEJ data set. Prominent features are two bands aligned with the dip equator, marking the position of the Appleton anomaly.

amplitudes up to 5 nT. Omitting this correction will cause systematic errors in the EEJ determination.

[18] Finally, the ring current and other magnetospheric current effects, as well as the quiet daily variations, Sq, were eliminated by fitting a degree-2 spherical harmonic polynomial with five internal ( $g_1^0, g_1^1, g_2^0, g_2^1, g_2^2$ ) and five external ( $q_1^0, q_1^1, q_2^0, q_2^1, q_2^2$ ) coefficients to the data orbit-by-orbit, similar to the procedure used by *Maus et al.* [2002] and then subtracting it. Measurements within a window of  $\pm 15^\circ$  centered on the dip equator have been omitted from the fitting procedure in order to avoid a feedback of the EEJ signal on the correction function.

[19] Figure 2 shows the superposition of the magnetic field signatures from all considered tracks centered at the dip equator. The position of the dip equator has been determined from the above mentioned main field model for an altitude of 108 km. The black curve represents the average residual magnetic field deflection after subtraction of a main and lithospheric field model and correction for the diamagnetic effect. The eastward EEJ current causes a reduction of the field strength. North and South of it there are indications for return currents. The EEJ is superimposed on the ring current and Sq magnetic signals, as has been reported earlier [e.g., *Onwumechili, 1967; Cain and Sweeney, 1973*]. This large-scale contribution, as determined by our fitting procedure, is plotted in Figure 2 as a gray band. The mean magnetic deflection amounts to  $-19$  nT and it peaks at the dip equator, as derived from the main field model. The positive deflections on the flanks are about a factor of 7 smaller.

[20] The amount of quantitative information on the EEJ, which can be drawn directly from the magnetic signature in total field is quite limited. Its width and amplitude depend strongly on the measurement height and the ambient field geometry. We regard the current density as a much more suitable parameter.

[21] To estimate the ionospheric current density, we assume a series of 81 east/west oriented line currents,  $0.5^\circ$  in latitude apart and located at an altitude of 108 km, where the EEJ current density is reported to peak [*Richmond, 1973a*].

[22] To account for the induction effect, we introduced in our model an identical series of mirror currents in the ground. This follows the approach of *Onwumechili and Ezema* [1992], who reported good results of their EEJ study when assuming a conductosphere below a depth of 200 km.

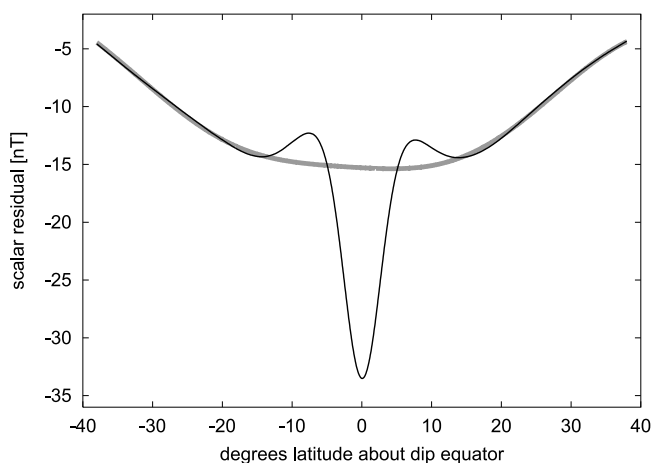


**Figure 2.** Average magnetic signature of the noon-time EEJ in the CHAMP scalar field readings. Displayed are the total external field contributions excluding the ring current, but including Sq currents and EEJ signatures (black line) and separately, the magnetic effect of the fitted large-scale ( $>10000$  km) current systems (gray band).

[23] The magnetic field caused by an eastward directed line current at orbital altitude can be written as follows:

$$b_x = -\frac{\mu_0 I}{2\pi} \frac{h}{x^2 + h^2}; \quad b_z = -\frac{\mu_0 I}{2\pi} \frac{x}{x^2 + h^2}, \quad (2)$$

where  $b_x$  and  $b_z$  are the northward and downward components of the magnetic field, respectively.  $I$  is the current strength,  $\mu_0$  the susceptibility of free space,  $h$  is the height above the current and  $x$  the northward displacement of the measurement point. The magnetic signature of the current in the field magnitude can be represented as

$$\Delta F = |\mathbf{B} + \mathbf{b}| - |\mathbf{B}|, \quad (3)$$

where  $\mathbf{B}$  is the unperturbed ambient field,  $\mathbf{b}$  the contribution of the current.

[24] The ambient magnetic field,  $\mathbf{B}$ , we derive from the above mentioned main field model. The  $\mathbf{B}$  has to be transformed into a frame, where the  $y$  component is aligned with the local direction of the EEJ and  $x$  is perpendicular to it, pointing predominantly northward.

[25] Since  $\mathbf{b}$  is much smaller than  $\mathbf{B}$  at orbital altitude, it is justified to replace equation (3) by the normalized dot product between  $\mathbf{B}$  and  $\mathbf{b}$ :

$$\Delta F = \frac{\mathbf{B} \cdot \mathbf{b}}{|\mathbf{B}|}. \quad (4)$$

[26] With this equation we obtain a linear relation between the total field deflection and the current strength. The intensities of each of the 81 considered independent line currents can be derived by linear inversion of the observed field residuals at the various satellite positions. We seek a solution with minimal second differences in adjacent line current strengths. Dividing the obtained current strength by the spatial distance between two lines gives the sheet current density.

[27] The employed infinitely long and straight currents do not reflect the actual geometry of the EEJ too well. For a first order correction we compared the magnetic effects of our line currents with a series of circularly shaped line currents matching the size of the Earth's ionosphere. We used a typical EEJ current profile (e.g., Figure 3) with eastward currents in the center and westward at the flanks. Current closure occurs in this model at the morning and evening terminators. The comparison of these two current models reveals for the typical altitude range of CHAMP,  $430 \pm 30$  km, that the line current geometry underestimates the current density by 11%. This factor has been applied to our estimates in order to make the obtained results directly comparable to other measurements, e.g., to ground observations.

### 2.1. Average Features of the Electrojet

[28] An inversion of the average EEJ magnetic signature of Figure 2 provides the latitudinal distribution of the current density, which is an average over all longitudes and seasons. The resulting current profile is shown in Figure 3. This graph gives a good impression of the mean characteristics of the noon-time electrojet. A prominent feature of the mean EEJ is among others the precise coincidence of the current peak with the dip equator. The return currents peak at latitudes of  $\pm 5^\circ$  on either side of the dip equator. This is

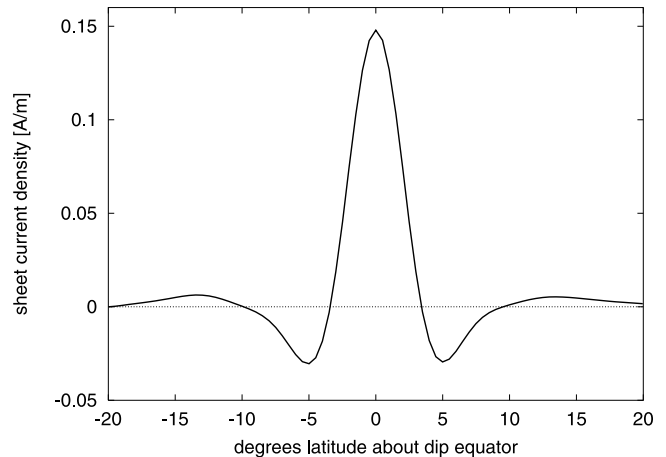


**Figure 3.** Average EEJ current density profile obtained by inverting the electrojet magnetic signature of Figure 2. The relative importance of the forward (positive) and return (negative) currents becomes obvious here.

significantly closer to the equator than suggested by the magnetic signature in Figure 2. The full width of the EEJ between the zero crossings of current density profile is  $6.8^\circ$  in latitude. Since the level of the zero current baseline is less well determined in the individual solutions, a more reliable measure is the width at half the peak value of the electrojet (hereafter termed *half-width*), which amounts to  $3.8^\circ$ . Encountered peak current densities are 0.15 A/m and  $-0.03$  A/m for the forward and return currents, respectively. The total average eastward current amounts to 65 kA. The return currents add up to 21 kA. At the noon-time we thus find a westward current which is about one third of the eastward EEJ.

### 3. Characteristics of the EEJ

[29] Having presented the average properties of the EEJ we now want to take a look at the variation of the electrojet features with longitude. In total, we have obtained 1653 latitude profiles. The distribution of the samples versus time can be seen in Figure 4. The intermittent availability of measurements is caused by the orbital precession of CHAMP through local time. Since we limit this study to the three hours around noon there are 33 consecutive days meeting the LT requirement followed by about 100 days outside the time window. Seasons have been marked by vertical lines in Figure 4.

[30] One of the most obvious features is the location of the peak current densities. Figure 5 (top) shows the dip latitude of each individual current peak versus longitude. The vast majority of maxima coincide within a fraction of a degree with the dip equator. The two dashed lines represent the 1 sigma uncertainty band of a running mean over  $20^\circ$  in longitude. There is no indication for a significant deviation of the EEJ from the dip equator at any longitude. In order to further test the significance of this statement, we have reordered the data. Figure 5 (bottom) shows the position of the EEJ peak versus the obtained peak current density. Here we clearly see that the scatter in the determined peak location is strongly related to the EEJ current density.

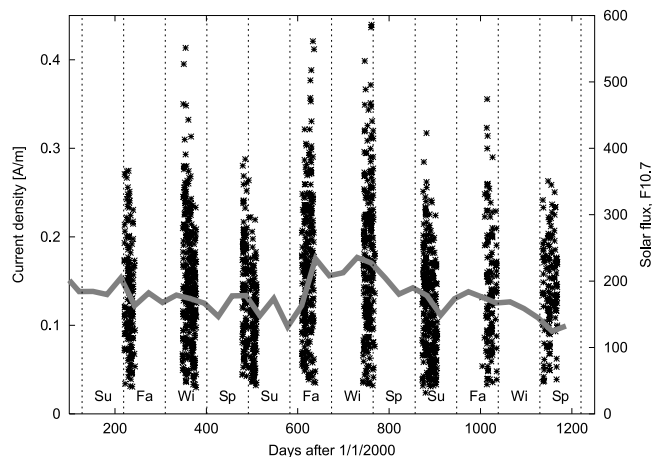


**Figure 4.** Dependence of the EEJ peak current density on the solar flux. The average current density tracks, in spite of its large variability, the level solar flux, F10.7, quite closely. Seasons have been separated by vertical lines. The intermittent availability of CHAMP noon-time data becomes evident in this figure.

Intense electrojets which can reliably be distinguished from other phenomena are mainly centered close to the dip equator. Current profiles exhibiting peak current densities of less than 30 mA/m have been rejected in our statistics, since they give quite unreliable results.

[31] Another spatial parameter is the width of the eastward current band. Figure 6 shows as asterisks (\*) the northern and southern latitude of the current density half-value width of all the profiles as a scatter plot. The majority of points are confined to bands at  $\pm 2^\circ$  latitudes showing little variation with longitude, which was also reported by *Ivers et al.* [2003]. The  $1\sigma$  scatter of these bands is on average  $0.2^\circ$ .

[32] Figure 6 also contains the northern and southern latitudes of the return current peaks (plus signs). They show a similar distribution with longitude as the current width. The return currents peak about  $5^\circ$  away from the dip equator.

[33] Another parameter of interest is the peak current density. This is a rather variable quantity, as can be seen from the scatter of the individual results in Figure 7. The day-to-day variability is enormous, even though we have considered only magnetically quiet days. In order to get an idea of the mean intensity at the various longitudes we have averaged the results in longitude bins. The solid curve is obtained by smoothing over a moving window of  $20^\circ$  longitude. The dashed lines represent the  $1\sigma$  spread. The mean height-integrated peak current density varies around 0.15 A/m. There are three distinct intensity peaks at about  $90^\circ\text{W}$ ,  $45^\circ\text{W}$ , and  $100^\circ\text{E}$  longitude. Between the prominent maxima there is a minimum at around  $50^\circ\text{E}$  longitude. The intensity changes by a factor of two between these extremes.

[34] It has often been noted, that the electrojet exhibits a seasonal variation in intensity. *Rastogi and Iyer* [1976] reported a semi-annual variation with maxima at the equinox and minima during solstice periods. For checking this statement we examine Figure 4. The individual groups of current density estimates show different average amplitudes. These follow quite closely the solar flux index, F10.7. There

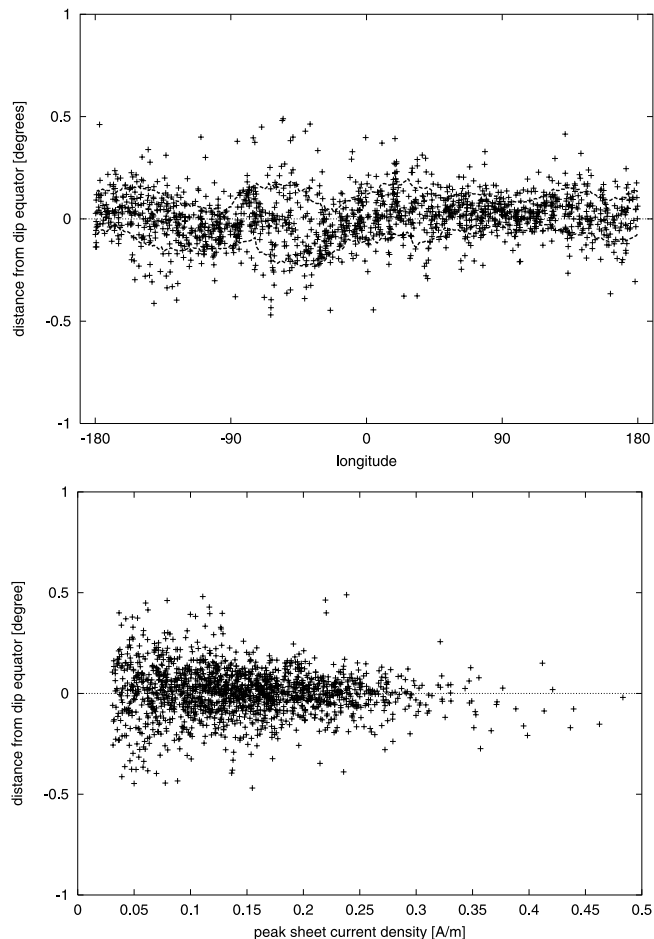


**Figure 5.** Position of the EEJ peak current density with respect to the dip equator. (top) Distribution of current peaks versus longitude. The dashed lines indicate the  $\pm 1\sigma$  uncertainty band. (bottom) Distribution of current peaks versus current intensity. For weak currents the estimated position is more uncertain.

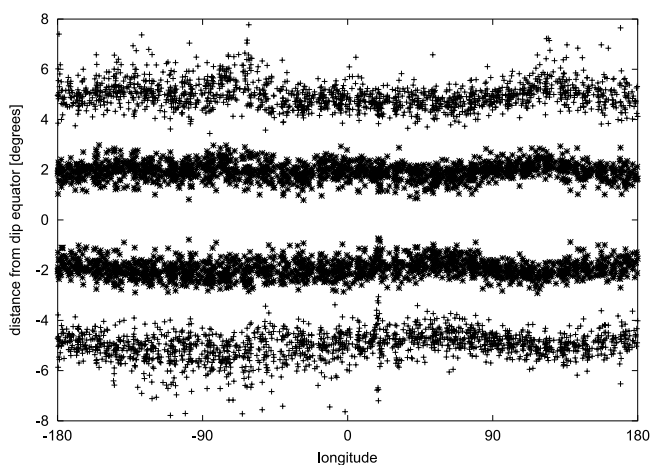


**Figure 6.** Variation of spatial EEJ features with longitude. Asterisks (\*) mark the latitudes where the electrojet reaches half its peak current density. The pluses (+) mark the latitude of the return current peaks. Both quantities show a similar dependence on longitude.

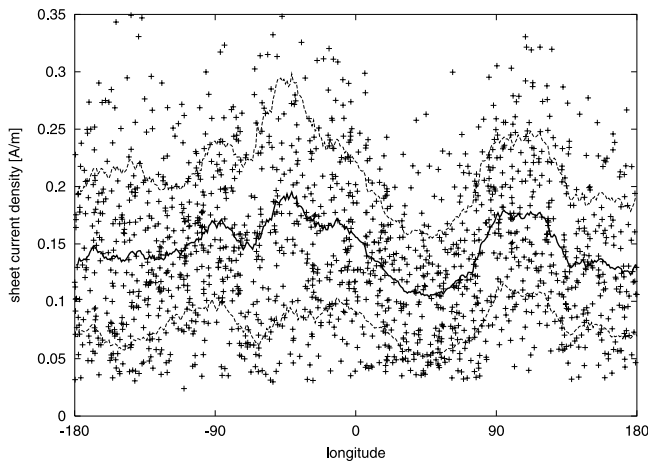


**Figure 7.** Variation of the EEJ peak current density with longitude. Data from all passes are included. The solid line represents a moving average over  $20^\circ$  longitude and the dashed lines indicate the  $\pm 1$  sigma band.

seems to be a close relationship between the short wavelength solar radiation and the EEJ intensity.

[35] During the time period considered the sun was rather active in Fall and Winter 2001 and somewhat higher flux occurred during Fall 2002. When binning our data set by seasons we get the largest current amplitudes in the late part of the year. This is in our eyes not a seasonal effect, but reflects the dependence of EEJ intensity on the solar flux.

[36] The distribution of the total forward (eastward) current with longitude, as shown in Figure 8 (full line), looks similar to the current density curve in Figure 7. The differences between minima and maxima are even more pronounced here. The integrated return (westward) current (dashed line) is significantly smaller and shows in some sectors the tendency of an anti-correlation.

[37] The quantity relating the total current and the current density is the width of the EEJ. Figure 9 shows a scatter plot of the half-width versus current density. There does not

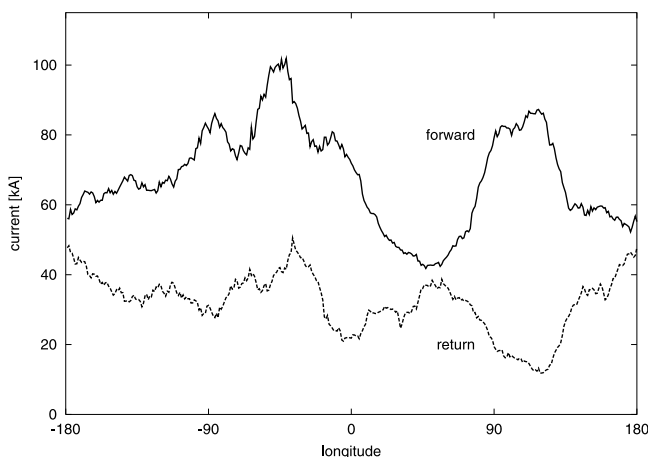


**Figure 8.** Variation of the total EEJ current with longitude. The curves of the forward (eastward) and return (westward) currents are obtained from a moving average over  $20^\circ$  longitude.

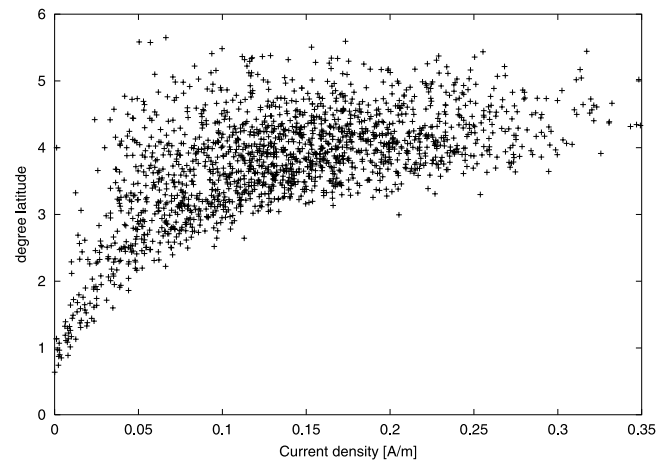


**Figure 9.** Distribution of the EEJ current half-width versus the peak current density. Higher current densities tend to occur in regions of wider current channels.

seem to be a strong correlation between the two quantities. We find, however, a certain trend indicating that high current densities go with larger widths. In any case, there is a kind of cut-off at the lower end. A certain peak current density obviously requires a minimum width.

[38] Our observation is in contrast to reports by *Onwumechili and Agu* [1981b], who claimed to have found an inverse trend, high current densities being associated with small widths. A similar trend is indicated by *Jadhav et al.* [2002, Figure 4]. Their results are in favor of conserving the total current intensity. This topic will be further detailed in the end of the discussion section 4.

[39] It has repeatedly been suggested that the width of the EEJ exhibits a seasonal variation. We could not confirm this statement. This could partly be due to the intermittent availability of our data, but in any case the effect cannot be prominent.

#### 4. Discussion

[40] In this section we want to revisit the results obtained in our extended study and discuss their consistency with characteristics of the EEJ, as reported in earlier papers.

[41] Our data selection is aiming at an identification of the primary features of the EEJ. We thus limited our attention to the three hours around noon, 10–13 LT, when the current system is expected to be most intense and symmetrical. Only low activity periods have been considered. CHAMP, due to its low orbit and its high resolution magnetometers, is particularly well suited to detect the details of the electrojet. The sizable number of passes, more than 1500, is a good basis for a comprehensive study. Particularly important for achieving significant results about the characteristics of the EEJ is, however, the proper removal of all other magnetic contributions coming from various sources. We paid special attention to this task which makes the obtained results unique and important compared to previous satellite studies of the noon-time EEJ.

[42] Both the employed main and lithospheric field models have been proven to be very reliable. In many of the previous EEJ studies from satellites [e.g., *Onwumechili*

and Agu, 1981a; Jadhav et al., 2002], lithospheric anomalies were not taken into account. Ivers et al. [2003] subtracted the nightside signatures from the dayside measurements to account for the lithospheric fields. Contributions from the large-scale current systems like Sq and the ring current have been removed in this study by fitting low order spherical harmonic functions, which are motivated by the geometry of the current systems, instead of removing them by filtering. This again makes a significant difference to earlier studies.

[43] Furthermore, the diamagnetic effect of plasma has been corrected for the first time. This effect causes significant reductions of magnetic field strength particularly in the dense plasma regions of the Appleton anomaly [Lühr et al., 2003]. Omitting this correction has a major impact on both the obtained EEJ current distribution and its intensity. Since the location and the peak density of the anomaly are closely related to the EEJ intensity, systematic errors will occur. For example, Rastogi and Iyer [1976] and Raghava Rao et al. [1988] have found a high correlation (0.85) of the equatorial plasma fountain intensity with the electrojet strength. This suggests that both belong to a coupled system.

[44] In the case of the CHAMP measurements, which have been sampled at an altitude around 430 km, the correction of the diamagnetic effect has an influence on several prime parameters of the EEJ. For example, the peak current density becomes larger by some 40%, the return currents are reduced by more than a factor of 2 and the longitude variation of the EEJ intensity is changed significantly.

[45] After these preprocessing steps we regard the remaining signal as entirely caused by the EEJ. It is thus justified to use a very general current model, such as a series of line currents, to invert the current distribution without any assumption on its form. This approach is quite different from earlier studies. Onwumechili [1997, pp. 144 and 277] deduced an empirical model of the EEJ current distribution based primarily on sounding rocket observations, but also adapted to satellite measurements. The formula for the current density contains a number of free parameters, which can be adjusted to obtain a best fit between the model and the magnetic field measurements. Jadhav et al. [2002] used this model and determined the free parameters by inverting the observations. Key parameters of the electrojet such as peak current density, current width or total current can then be deduced from this model as analytical functions depending only on the determined free parameters. Unfortunately, the inversion of Jadhav et al. [2002] seems to be flawed, since they equated the magnetic effect in the total field to the root of the sum of the squared horizontal and vertical components ( $\Delta F = \sqrt{x^2 + z^2}$ ). Actually, the change in total field is equal to the normalized dot product between the ambient field and the magnetic effect of the current (see equation (4)). Making use of a dedicated current model has advantages, if the data are contaminated by some unknown effects, but on the other hand there is the danger of deriving biased results.

[46] A primary feature of the EEJ is the latitude of the current peak. As can be seen in Figure 5 (top), the peak current density is reached at the dip equator. This result is consistent with the findings of Fambitakoye and Mayaud [1976]. The encountered scatter about that position is inversely proportional to the current intensity. Figure 5

(bottom) provides probably an impression on the uncertainty involved in our method to determine automatically the peak location. A similar scatter plot was presented by Jadhav et al. [2002, Figure 4e]. It has also been indicated earlier that a strong EEJ deviates less from the dip equator [Fambitakoye and Mayaud, 1976]. Furthermore, Jadhav et al. [2002] showed that the EEJ axis is found closest to the dip equator at noon, the time sector we have investigated.

[47] We observe no systematic variation of the proximity between EEJ axis and dip/equator with longitude. This finding is in line with reports of Onwumechili and Agu [1980] but in contrast with results of Jadhav et al. [2002], who analyzed Ørsted satellite data and reported a deviation of the EEJ center from the dip equator of up to  $0.7^\circ$  at certain longitudes. A possible explanation for the apparent discrepancy could be that the magnetic field model used by them, the IGRF 2000, is not accurate enough and does not remove influences of small-scale sources sufficiently.

[48] The seasonal variation of the electrojet axis, as suggested by Gupta [1973], we also cannot confirm. Already Forbes [1981] had argued that the apparent shift of the EEJ axis reported by this author could be caused by an imperfect separation of the large-scale  $S_q$  variation from the electrojet signature.

[49] Another parameter we have investigated is the width of the electrojet. From Figure 3 it is obvious that the width can be defined in different ways. One could either consider only the forward current or take also the return currents into account. We have taken the half-width of the forward current. As shown in Figure 6, the average EEJ width is about  $4^\circ$  in latitude and varies only approximately  $\pm 10\%$  over all longitudes. Larger widths are found over Indonesia ( $120^\circ\text{E}$ ) and the eastern Pacific ( $120^\circ\text{W}$ ). Over Africa the EEJ is narrower. Although many of the previous studies [e.g., Onwumechili, 1967; Jadhav et al., 2002] find a maximum width over South America, we cannot confirm it and also Ivers et al. [2003] do not find it. The reason for the enhanced width may be a geometrical effect. In this sector the EEJ flows at an angle of  $30^\circ$  with respect to the eastward direction. We have calculated the width perpendicular to the stream lines instead of taking due the north direction. A day-to-day variation of the electrojet width of some 20%, as reported by Burrows [1970], is not consistent with our observations.

[50] An important quantity is the current density distribution with latitude. Since we perform our magnetic field measurements well above the current carrying E layer, it is justified to approximate it by a sheet current at 108 km altitude. With an average height-integrated peak current density of 0.15 A/m (see Figure 7) we are somewhat lower than previously published results. Other researchers report current densities around 0.2 A/m [e.g., Onwumechili and Agu, 1981b; Jadhav et al., 2002]. A possible explanation for this difference might be the current models used (as mentioned above) when inverting the magnetic signatures.

[51] As a test, we calculated the EEJ current density relative to a somewhat arbitrary baseline, a tangent attached to the shoulders in the magnetic residual signal, both sides of electrojet signature (see Figure 2). The upper curve in Figure 10 shows the peak current density derived with the new baseline. These current intensities can be determined very reliably. They are on average 0.19 A/m, which is close to the value of Jadhav et al. [2002]. They can be regarded as

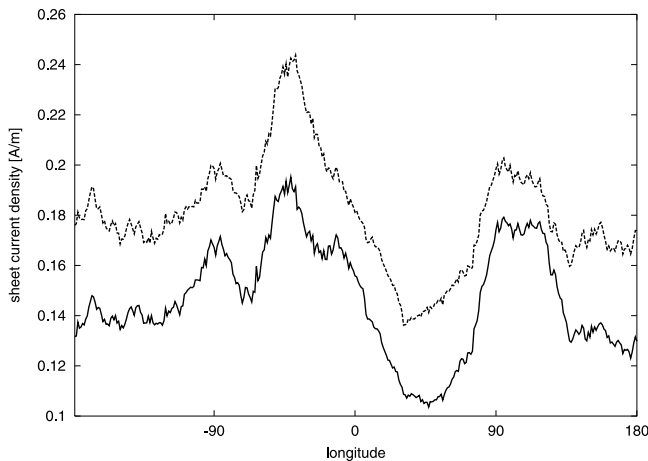


**Figure 10.** Smoothed peak current density variations with longitude. The lower curve (full line) represents the results from this study. The upper curve (broken line) reflects the current densities, if return currents are suppressed (for details see text).

upper limits. The lower curve repeats our peak currents densities estimates, as shown in Figure 7. In both cases the individual results are averaged over  $20^\circ$  in longitude. The two curves track each other quite closely. This adds confidence to our automatically determined baseline and the resulting variation with longitude.

[52] There have been reports about large variations in current intensity with altitude, producing an exponentially decaying sinusoidal function for the EEJ magnetic signature with altitude [e.g., *Onwumechili and Agu*, 1980]. Since CHAMP is circling the Earth on an almost circular orbit, we could not check the validity of this peculiar effect. A possible reason could, however, be the diamagnetic effect.

[53] A persistent feature present in all our profiles are the return currents on the flanks of the electrojet peaking at latitudes of about  $\pm 5^\circ$  on either side of the dip equator and exhibiting a distinct variation with longitude (see Figure 6). Although not mentioned in most studies based on ground-based observations and sometimes even called into question [e.g., *Stening*, 1995], the return currents are a clearly visible feature in magnetic field recordings from low flying satellites [e.g., *Cain and Sweeney*, 1973].

[54] It has to be mentioned here that the obtained intensity of the return currents depends strongly on the proper correction of the diamagnetic effect. As mentioned in section 2, we have used a constant value of 2000 K for the sum of ion and electron temperatures when calculating the plasma pressure. There may well be systematic temperature variations related to the Appleton anomaly. These would give rise to a somewhat modified baseline. As long as the plasma temperatures and densities are not measured simultaneously with the magnetic field, the role of the return currents cannot be determined unambiguously.

[55] A feature of the EEJ which has been of interest for quite a while is the intensity variation with longitude. It is difficult to obtain a global picture from ground observations alone, because large parts of the electrojet are over oceans. Satellite measurements with their global coverage are much better suited for this task. A further complication arises from

the enormous day-to-day variability of the current intensity (see Figure 7). A large number of samples is required to obtain statistically significant results. EEJ intensity variations with longitude based on POGO measurements were published by *Onwumechili and Agu* [1981a] and on Ørsted measurements by *Jadhav et al.* [2002]. *Ivers et al.* [2003] deduced relative EEJ intensities from Ørsted scalar magnetic field signatures. Although the results from the three satellite missions look quite different in detail, they do have certain features in common. Our secondary peak at  $100^\circ\text{E}$  longitude is present in all data sets. The peak at the west coast of South America,  $280^\circ\text{E}$ , is also present in our data. However, our prime peak at  $45^\circ\text{W}$  is not well reflected in their plots. Over the Pacific,  $190^\circ\text{E}$ , a secondary peak emerges in the POGO and Ørsted measurements, while we see a fairly low intensity throughout the Pacific. Our minimum at  $40^\circ\text{E}$  is present in the Ørsted results, but not well reflected in the POGO data. *Langel et al.* [1993] studied the evening electrojet using Magsat data. They found a maximum in intensity over south America and a minimum in the area of Indonesia where we have a maximum.

[56] Obviously, the intensity variation of the electrojet with longitude is also dependent on local time. Since we have limited our investigations to the hours around noon, no statements can be made on the local time dependence.

[57] A number of possible causes for the longitude variation of the electrojet strength have been suggested [e.g., *Forbes* 1981]. Most obvious seems to be the dependence of the Cowling conductivity on the ambient field strength. Another possible cause is the angle between the orientation of the dip equator and the ambient magnetic field. It deviates in some regions by  $12^\circ$  from orthogonality. That means, the EEJ current has a non-vanishing component parallel to the lines of force. The parallel conductivity is known to be very high, thus currents can be more intense here, if we assume the same electric field strength. Furthermore, the EEJ deviates from the geographic equator by up to  $12^\circ$  in latitude, and the currents flow in some regions at an angle of  $30^\circ$  with respect to the east-west direction. This may change the influence of zonal winds either in favor of or opposing the plasma motion. The global east-west electric field is to a certain extent controlled by the cross-polar cap potential. Its influence gets smaller toward lower latitudes [*Kobea et al.*, 2000]. The distance to either of the corrected geomagnetic poles could thus have an effect on the current strength, in particular when the EEJ flows at a certain distance from the symmetry line between the two magnetic poles. At  $60^\circ\text{W}$  longitude it is  $12^\circ$  closer to the north magnetic pole and at  $120^\circ\text{E}$  about  $12^\circ$  closer to the southern pole. In Figure 11 the variations of all these quantities with longitude have been plotted. Most of the mentioned parameters show a poor relation to the EEJ intensity maxima. Just the bottom plot provides a reasonable correlation with the current density. The proximity to any of the magnetic poles seems to be in favor of an enhanced EEJ intensity.

[58] Finally, we have a look at the total current integrated over latitude. Figure 8 shows the variation of the total current with longitude separately for the forward (eastward) and return (westward) currents. The strength of the eastward current varies around an average of some 65 kA. This is a value consistent with earlier reports.

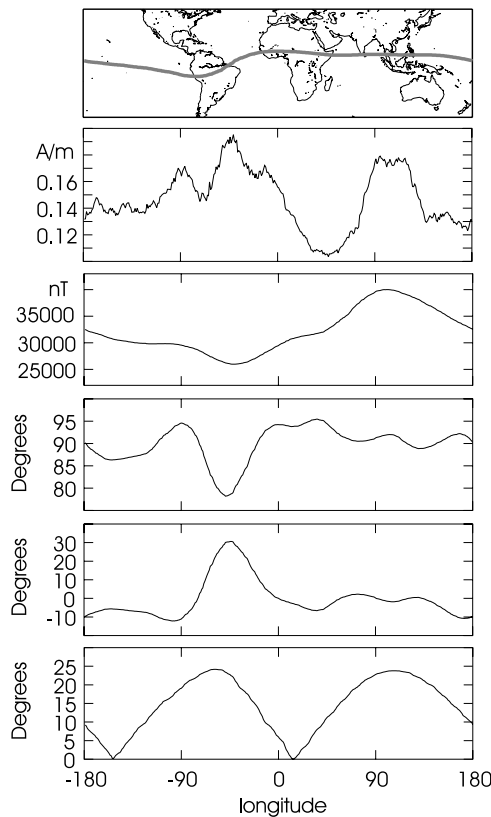


**Figure 11.** Variation of several quantities with longitude, which could control the intensity of the EEJ. From top to bottom: location of the EEJ in the various parts of the world, distribution of the average EEJ peak current density, magnetic field intensity, angle between the ambient magnetic field and the EEJ current, angle between the EEJ and geographic east, and difference in great circle distance of the EEJ to the corrected geomagnetic north and south poles.

[59] The return currents sum up to an average of 26 kA. It has to be pointed out, however, that the obtained results for the return current depend strongly on the diamagnetic correction applied. We thus would not like to get too far in the interpretation of its variation with longitude.

[60] In section 3 it has been noted that the total eastward current and the average EEJ peak current density (see Figures 8 and 10) exhibit a similar variation with longitude. We wanted to explore this relation a little further and plotted in Figure 12 the smoothed total current versus the peak current density on a log-log scale. As can be seen in the figure, the relationship is reasonably linear. This tells us that the total current is related to current density by a power law. From the regression line we read the relation:

$$I_{\text{total}}[\text{kA}] = 938.5(j_{\text{peak}}[\text{A/m}])^{1.38}. \quad (5)$$

[61] The quantity relating the total current and the current density is the width of the electrojet channel. Since we find an exponent larger than 1, it has to be concluded that high current densities are accompanied by wider channels. This is consistent with our statement in section 3 on the relation between current density and width (see Figure 9).

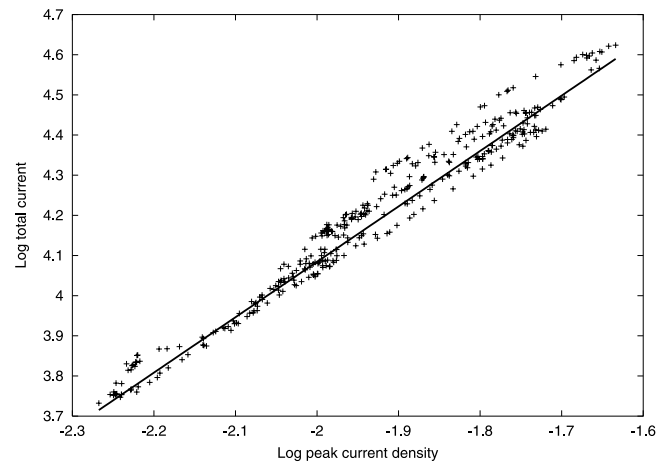


**Figure 12.** Ratio between EEJ total forward current and peak current density. On a log-log scale both show a close linear relation.

[62] In the above analysis we have used current data averaged over time in each longitude bin. One can also reverse the procedure and look at the temporal variations in a fixed longitude bin. We have repeated the above exercise using all individual samples in the longitude range  $80^\circ$  to  $120^\circ\text{E}$ . The fitting procedure, shown in Figure 13, gives an exponent for the current density of 1.18. This means that the total current and current density are almost directly proportional.

[63] From these results we may draw different conclusions for temporal and spatial variation of the EEJ. Looking at the dependence on longitude we find a power law relation between the total current and current density. This could be explained by a fixed relation between the meridional width of the Cowling channel and the current slab thickness. The latter is giving rise to an enhanced height-integrated current density for wider electrojets. Under this aspect the variation of the EEJ intensity with longitude can be explained entirely

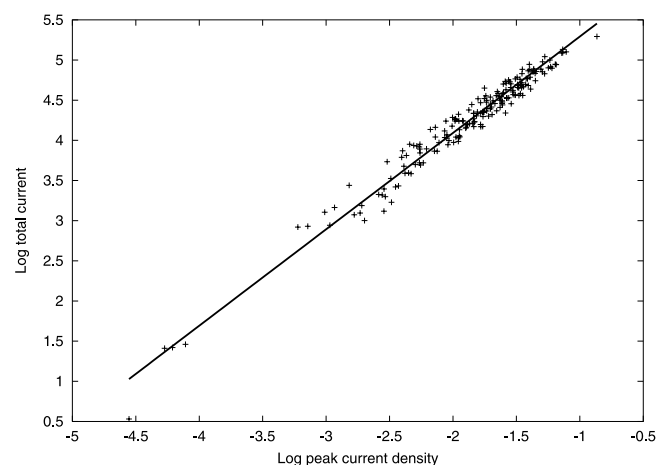


**Figure 13.** Ratio between smoothed EEJ total forward current and peak current density for each individual sample within the longitude sector  $80^\circ$ – $120^\circ\text{E}$ . The slope of the regression line is almost one on the log-log scale.

by its geometry. At longitudes with larger cross-sections of the Cowling channel larger currents can flow under the same environmental conditions.

[64] When analyzing data from a fixed longitude the obtained linear relation between total current and current density implies a constant width not depending on the intensity. It was already suggested in section 3 that locally the geometry of the Cowling channel is fairly constant, independent of the enormous temporal variation of the EEJ intensity. For a more reliable distinction between temporal and spatial variation it would, however, be better to look at observations from more than one spacecraft simultaneously.

## 5. Summary

[65] We have presented a comprehensive study of the noon-time equatorial electrojet. Due to the good quality of the CHAMP magnetic field measurements and to significant improvements in field separation, highly reliable results have been obtained. The magnetic field variations were interpreted in terms of ionospheric currents from which the EEJ characteristics are deduced.

[66] Some of the special features are listed here:

[67] 1. The noon-time EEJ current peaks precisely at the dip equator, given by an accurate main field model at 108 km altitude. This is valid for all longitudes and seasons.

[68] 2. The half-width of the EEJ (about 4° in latitude) is rather constant in time at a given longitude, independent of intensity. The variation with longitude amounts to ±10%.

[69] 3. The noon-time EEJ current density profiles exhibit a sharp peak at the dip equator. There are enormous day-to-day intensity variations. The average peak current density is about 0.15 A/m. It is closely related to the amount of solar flux. A possible seasonal variation is obscured by the changes in F10.7.

[70] 4. There is a systematic variation of peak current density with longitude. Regions of enhanced current strength appear around longitudes of 60°W and 100°E. An absolute minimum is attained at 40°E.

[71] 5. Consistent features are the return currents on the northern and southern flanks. They peak at an average distance of about 5° from the dip equator.

[72] 6. The total EEJ current amounts on average to 65 kA. The variation of the current strength with longitude is very similar to that of the current density.

[73] 7. From a comparison between the total current and the current density we derive the suggestion that the longitude variation of the EEJ intensity can be explained by differences in cross-section of the Cowling channel.

[74] The presented observations could not answer all of the open questions. These should be addressed in follow-up studies. A direct comparison of our current profiles with concurrent ground-based measurements could be one of the next steps.

[75] **Acknowledgments.** The operational support of the CHAMP mission by the German Aerospace Center (DLR) and the financial support for the data processing by the Federal Ministry of Education and Research (BMBF) are gratefully acknowledged. This study was performed as part of the DFG Priority Program "Geomagnetic Variations," SPP1097.

[76] Arthur Richmond thanks Geeta Jadhav and another reviewer for their assistance in evaluating this paper.

## References

- Ananda Rao, B., and R. Raghava Rao (1987), Structural changes in the current fields of the equatorial electrojet due to zonal and meridional winds, *J. Geophys. Res.*, *92*, 2514–2526.
- Burrows, K. (1970), The day-to-day variability of the equatorial electrojet in Peru, *J. Geophys. Res.*, *75*, 1319–1323.
- Cain, J., and R. Sweeney (1973), The POGO data, *J. Atmos. Terr. Phys.*, *35*, 1231–1247.
- Cowling, T. (1933), The electrical conductivity of an ionized gas in the presence of a magnetic field, *Mon. Not. R. Astron. Soc.*, *93*, 90–98.
- Fambitakoye, O., and P. Mayaud (1976), Equatorial electrojet and regular daily variation SR; II, the center of the equatorial electrojet, *J. Atmos. Terr. Phys.*, *38*, 19–26.
- Fambitakoye, O., P. Mayaud, and A. Richmond (1976), Equatorial electrojet and regular daily variation *s*, III, Comparison of observations with a physical model, *J. Atmos. Terr. Phys.*, *38*, 113–121.
- Forbes, J. M. (1981), The equatorial electrojet, *Rev. Geophys.*, *19*, 469–504.
- Gupta, J. (1973), Movement of the  $S_q$  foci in 1958, *Pure Appl. Geophys.*, *110*, 2076–2084.
- Ivers, D., R. Stening, J. Turner, and D. Winch (2003), Equatorial electrojet from Ørsted scalar magnetic field observations, *J. Geophys. Res.*, *108*(A2), 1061, doi:10.1029/2002JA009310.
- Jadhav, G., M. Rajaram, and R. Rajaram (2002), A detailed study of equatorial electrojet phenomenon using Ørsted satellite observations, *J. Geophys. Res.*, *107*(A8), 1175, doi:10.1029/2001JA000183.
- Kobe, A., A. Richmond, B. Emery, C. Peymirat, H. Lühr, T. Moretto, M. Hairston, and C. Amory-Mazaudier (2000), Electrodynamic coupling of high and low latitudes: Observations on May 27, 1993, *J. Geophys. Res.*, *105*, 22,979–22,989.
- Köhnlein, W. (1986), A model of the electron and ion temperatures in the ionosphere, *Planet. Space Sci.*, *34*, 609–630.
- Langel, R. A., M. Purucker, and M. Rajaram (1993), The equatorial electrojet and associated currents as seen in Magsat data, *J. Atmos. Terr. Phys.*, *55*, 1233–1269.
- Lühr, H., M. Rother, S. Maus, W. Mai, and D. Cooke (2003), The diamagnetic effect of the equatorial Appleton anomaly: Its characteristics and impact on geomagnetic field modeling, *Geophys. Res. Lett.*, *30*(17), 1906, doi:10.1029/2003GL017407.
- Maus, S., M. Rother, R. Holme, H. Lühr, N. Olsen, and V. Haak (2002), First scalar magnetic anomaly map from CHAMP satellite data indicates weak lithospheric field, *Geophys. Res. Lett.*, *29*(14), 1702, doi:10.1029/2001GL013685.
- Onwumechili, C. (1967), Geomagnetic variation in the equatorial zone, in *Physics of Geomagnetic Phenomena*, edited by W. Matsushita and S. Campbell, pp. 425–507, Academic, San Diego, Calif.
- Onwumechili, C. A. (1997), *The Equatorial Electrojet*, Gordon and Breach, Newark, N. J.
- Onwumechili, C., and C. Agu (1980), General features of the magnetic field of the equatorial electrojet measured by the POGO satellites, *Planet. Space Sci.*, *28*, 1125–1130.
- Onwumechili, C. A., and C. E. Agu (1981a), Longitudinal variation of equatorial electrojet parameters derived from POGO satellite observations, *Planet. Space Sci.*, *29*, 627–634.
- Onwumechili, C. A., and C. E. Agu (1981b), The relationship between the current and the width of the equatorial electrojet, *J. Atmos. Terr. Phys.*, *43*, 573–578.
- Onwumechili, C. A., and P. O. Ezema (1992), Latitudinal and vertical parameters of the equatorial electrojet from an autonomous data set, *J. Atmos. Terr. Phys.*, *54*, 1535–1544.
- Raghava Rao, R., R. Sridharan, J. Sastri, V. Agashe, B. Rao, P. Rao, and V. Somajajula (1988), The equatorial ionosphere, in *WITS Handbook*, vol. 1, *World Ionosphere/Thermosphere Study*, edited by C. H. Liu and B. Edwards, pp. 48–93, Univ. of Ill., Urbana.
- Rastogi, R. G. (1989), The equatorial electrojet, in *Geomagnetism*, vol. 3, edited by J. Jacobs, pp. 461–525, Academic, San Diego, Calif.
- Rastogi, R. G., and K. N. Iyer (1976), Quiet day variation of geomagnetic H field at low latitudes, *J. Geomagn. Geoelectr.*, *28*, 461–478.
- Richmond, A. D. (1973a), Equatorial electrojet-1. Development of a model including winds and instabilities, *J. Atmos. Terr. Phys.*, *35*, 1083–1103.
- Richmond, A. D. (1973b), Equatorial electrojet-2. Use of the model to study the equatorial ionosphere, *J. Atmos. Terr. Phys.*, *35*, 1105–1118.
- Stening, R. J. (1995), What drives the equatorial electrojet?, *J. Atmos. Terr. Phys.*, *57*, 1117–1128.
- H. Lühr, S. Maus, and M. Rother, GeoForschungsZentrum Potsdam, Telegrafenberg, D-14473 Potsdam, Germany. (hluehr@gfz-potsdam.de)